

Intermittent transport in edge plasmas

O. E. Garcia, V. Naulin, A. H. Nielsen, and J. Juul Rasmussen
Association EURATOM-Risø National Laboratory
Optics and Plasma Research, OPL-128 Risø
DK-4000 Roskilde, Denmark

Abstract

The properties of low-frequency convective fluctuations and transport are investigated for the boundary region of magnetized plasmas. We employ a two-dimensional fluid model for the evolution of the global plasma quantities in a geometry and with parameters relevant to the scrape-off layer of confined toroidal plasmas. Strongly intermittent plasma transport is regulated by self-consistently generated sheared poloidal flows and is mediated by bursty ejection of particles and heat from the bulk plasma in the form of blobs. Coarse grained probe signals reveal a highly skewed and flat distribution on short time scales, but tends towards a normal distribution at large time scales. Conditionally averaged signals are in perfect agreement with experimental measurements.

It is well established that the cross field transport of particles and heat near the edge of magnetically confined plasmas is strongly intermittent. This is observed in a variety of devices including linear [1, 2] as well as toroidal configurations [3, 4]. Detailed investigations of the spatial fluctuation structure have revealed strong indications that the intermittent nature of particle and heat transport is caused by localized structures in the form of plasma “blobs” propagating radially far into the scrape-off-layer (SOL) of toroidal plasmas [2, 5, 6]. It was suggested that this is caused by a dipolar vorticity field formed by the charge separation in a density blob due to guiding-center drifts in a curved inhomogeneous magnetic field [7].

In this contribution we will provide a self-consistent description of the intermittent particle and heat flux and link it to the emergence and evolution of such blob-like structures. We base our investigations on a novel model for interchange turbulence in slab geometry for the outboard midplane of a toroidal device [8]. The model includes the self-consistent evolution of the full profiles in the edge/SOL. A local Boussinesq-like model, where the “background” profile is separated from the fluctuations, fails to provide a realistic description. The geometry comprises distinct production and loss regions, corresponding to the edge and SOL of magnetized plasmas. The separation of these two regions defines an effective last closed flux surface (LCFS), though we do not include magnetic shear in our model. In the edge region, strong pressure gradients maintain a state of turbulent convection. A self-regulation mechanism involving differential rotation leads to a repetitive expulsion of hot plasma into the SOL, resulting in a strongly intermittent transport of density and heat.

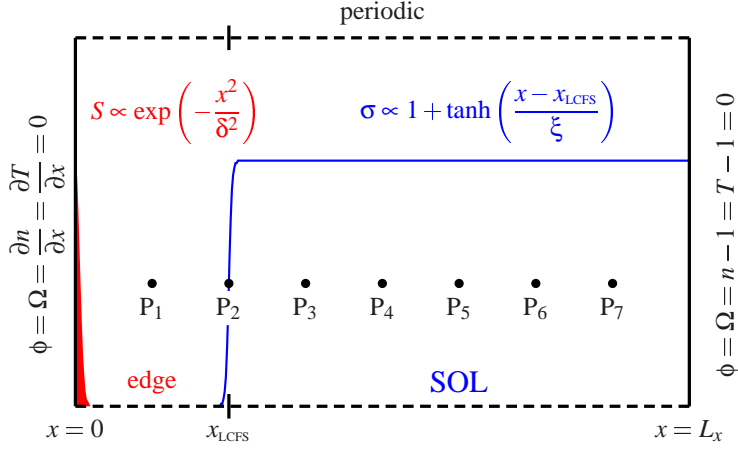


Figure 1: Geometry of the simulation domain showing the forcing region to the left, corresponding to the edge plasma, and the parallel loss region to the right, corresponding to the scrape-off layer. Parameters are $\delta = 8$ and $\xi = 1$. Data time series are collected at the probe positions P_i .

The model derives from the continuity equations for the electrons, the electron temperature and the quasi-neutrality condition. Assuming cold ions and neglecting electron inertia effects, we obtain a three-field model for electrostatic perturbations of the full particle density n , electric potential ϕ and electron temperature T . Using slab coordinates with $\hat{\mathbf{z}}$ along the magnetic field, $\hat{\mathbf{x}}$ in the radial and $\hat{\mathbf{y}}$ in the poloidal direction we obtain [8],

$$\begin{aligned} \frac{d\Omega}{dt} - C(p) &= v_\Omega \nabla^2 \Omega - \sigma_\Omega \Omega, \\ \frac{dn}{dt} + nC(\phi) - C(nT) &= v_n \nabla^2 n - \sigma_n (n - 1) + S_n, \\ \frac{dT}{dt} + \frac{2T}{3} C(\phi) - \frac{7T}{3} C(T) - \frac{2T^2}{3n} C(n) &= v_T \nabla^2 T - \sigma_T (T - 1) + S_T, \end{aligned}$$

where time is normalized by $1/\omega_{ci}$ and spatial scales by $\rho_s = c_s/\omega_{ci}$. The density n and temperature T are normalized to fixed characteristic values at the outer wall. We further define the advective derivative, the magnetic field curvature operator and the toroidal magnetic field by

$$\frac{d}{dt} = \frac{\partial}{\partial t} + \frac{1}{B} \hat{\mathbf{z}} \times \nabla \phi \cdot \nabla, \quad C = -\zeta \frac{\partial}{\partial y}, \quad B = \frac{1}{1 + \varepsilon + \zeta x}.$$

The vorticity $\Omega = \nabla_\perp^2 \phi$, the inverse aspect ratio $\varepsilon = a/R_0$ and $\zeta = \rho_s/R_0$ where a and R_0 are the minor and major radius of the device. The terms on the right hand side of the equations describe external sources S , parallel losses along open field lines through the damping rates σ [8], and collisional diffusion with coefficients v . The geometry and boundary conditions are sketched in Fig. 1.

In the absence of external forcing and dissipative processes the model equations non-linearly conserves the global energy to lowest order in ζ

$$E = \int d\mathbf{x} \left[\frac{1}{2} (\nabla_\perp \phi)^2 + \frac{3}{2} nT \right],$$

where the integral extends over the whole plasma layer. We define the kinetic energy of the fluctuating and mean components of the flows,

$$K = \int d\mathbf{x} \frac{1}{2} (\nabla_{\perp} \tilde{\phi}), \quad U = \int d\mathbf{x} \frac{1}{2} v_0^2, \quad (1)$$

where the zero index denotes an average over the periodic direction y and the spatial fluctuation about this mean is indicated by a tilde. The linearly damped mean flows, $v_0 = \partial\phi_0/\partial x$, does not yield any radial convective transport and hence form a benign path for fluctuation energy. The energy transfer rates from thermal energy to the fluctuating motions, and from the fluctuating to the mean flows, are given respectively by

$$F_p = \int d\mathbf{x} nT C(\phi), \quad F_v = \int d\mathbf{x} \tilde{v}_x \tilde{v}_y \frac{\partial v_0}{\partial x}. \quad (2)$$

Note that F_p is directly proportional to the domain integrated convective thermal energy transport, while F_v shows that structures tilted such as to transport positive poloidal momentum up the gradient of a sheared flow will sustain the flow against collisional dissipation [9, 10, 11].

In the following we present results from numerical simulations of the interchange model using parameters relevant for SOL plasmas. $L_x = 2L_y = 200$ and the LCFS is located at $x_{\text{LCFS}} = 50$. The parameters are $\varepsilon = 0.25$, $\zeta = 5 \times 10^{-4}$, and $\nu = 10^{-2}$ for all fields. The parallel loss rate of temperature is assumed to be five times larger than that on the density and vorticity, $\sigma_n = \sigma_{\Omega} = \sigma_T/5 = 3\zeta/2\pi q$, since primarily hot electrons are lost through the end sheaths. σ_n and σ_{Ω} correspond to losses at the nearest target plate over a distance of $L_{\parallel} = 2\pi R_0 q/3$ (one third of the connection length) with the acoustic speed c_s , where $q = 3$ is the safety factor at the edge. Finally, the radial line-integral of the sources S_n and S_T equals 0.1. For the numerical solution the spatial resolution is 512×256 grid points in the radial and poloidal directions, and the time span of the simulation is 2×10^6 .

We have performed several runs with varying parameters, showing that the qualitative behavior is robust, whereas the quantitative results depend on the parameters and particular on the value of the collisional diffusivities. The general observation is that the turbulent flux is strongly intermittent: quiet periods are interrupted by strong bursts of particle and heat fluxes. This is correlated with the kinetics in the fluctuations, as is shown in Fig. 2. We observe that the convective energy and thermal transport appears as bursts during which particles and heat are lost from the edge into the SOL region. As discussed in Refs. [9, 10, 11], this global dynamics is caused by a self-regulation mechanism in which kinetic energy is transferred from the fluctuating to the mean components of the flows, and subsequently damped by collisional dissipation. The thermal energy ejected in a bursty manner from the edge and into the SOL region, will eventually be lost by transport along open field lines. The characteristic time between the bursts is related to the viscous diffusion (compare with Fig. 3 in Ref. [8], where the value of ν is 5×10^{-3}). We further verified that the self-sustained poloidal flow profiles are strongly sheared in the edge region, and have larger amplitudes during the strong fluctuation period.

The statistics of single-point recordings at different radial positions P_i indicated in Fig. 1 agree very well with experimental measurements. In Fig. 3 we present the probability distribution functions (histogram of counts) (PDF) of the density signals taken from a long-run simulation

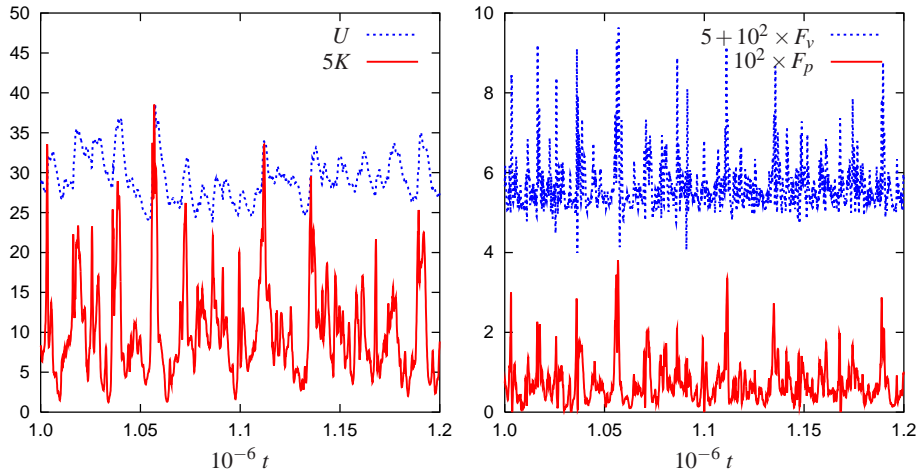


Figure 2: Evolution of the kinetic energy contained by the mean U and fluctuating K motions [Eq. (1)] and the collective energy transfer terms [Eq. (2)] .

containing more than a hundred strong burst events. It is notably that the PDF at the first probe inside the LCFS is close to a Gaussian with skewness 0.12 and flatness factor 2.97, while the PDF becomes more flat and skewed further into the SOL. This indicates the high probability of large positive fluctuations corresponding to blobs of excess plasma. The skewness and flatness factors grow through out the SOL and take values up to 4 and 25, respectively. The PDF's in the SOL have similar structure with a pronounced exponential tail towards large values, a characteristic feature of turbulent convection in the presence of sheared flows [9, 10].

We have also considered the coarse-grained PDF which is obtained by averaging the signal over time intervals of lengths τ and constructing new time records with a time resolution of τ : $n_\tau(t) = (1/\tau) \int_{t-\tau/2}^{t+\tau/2} n(t') dt'$. The coarse grained PDF's (PDF $_\tau$) for the signal at P_3 are also plotted in Fig. 3 for increasing values of τ . We observe that PDF $_\tau$ approaches a Gaussian distribution when τ is exceeding the averaged time interval between bursts, which is roughly 10^4 . This shows the absence of self-similarity, which is characteristic for an intermittent signal (see, e.g., [12]).

The conditionally averaged temporal wave forms of the density calculated from the same signals and the radial velocity field v_x , using the trigger condition $n - \bar{n} > 4n_{\text{rms}}$ at each individual point, are presented in Fig. 4. For the density signal an asymmetric wave form with a sharp rise and a relatively slow decay is clearly seen, as also observed in experimental measurements [2, 5, 6]. The maximum density excursions significantly exceed the background level, and decay as the structures propagate through the SOL. By using a negative amplitude for the conditional averaging very few realizations results, confirming the presence of blob-like structures. For the velocity signal we observe that the radial velocity is positive (directed radially outwards) in the blob. In the edge region it takes weak negative values both before and after the blob. Also this result agree with experimental observations [5]. We note that the maximum value of v_x decreases on passing the LCFS and then increases to a maximum value of 0.046 at P_3 , after which it slowly decays. From two-dimensional animations we clearly observe the radial propagation of

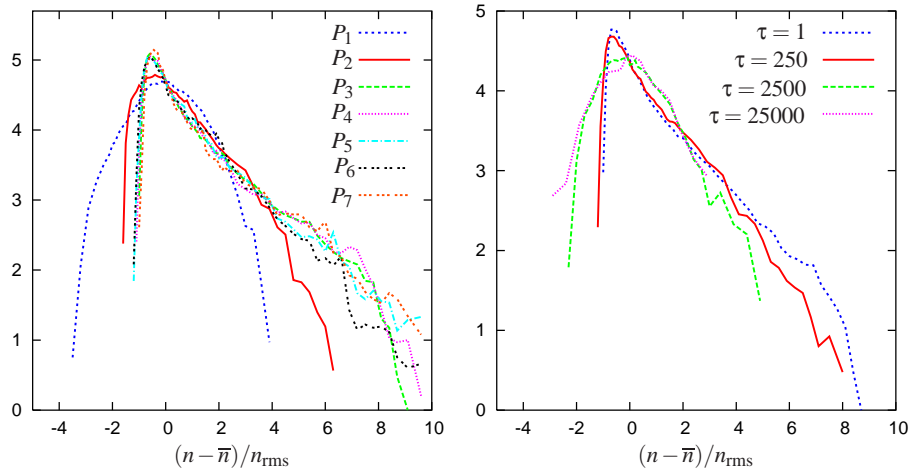


Figure 3: In the left panel is shown the probability distribution functions of particle density measured at seven different radial positions P_i as shown in Fig. 1. To the right is the coarse grained probability distribution function taken at probe 3, averaged over the time intervals τ indicated by the labels. With increasing τ the skewness decreases as: 2.6, 1.9, 0.73, 0.16, and the flatness factor decreases as: 12.0, 7.8, 3.9, 3.2. For both plots the vertical axis shows count numbers on a logarithmic scale. \bar{n} designates the averaged density.

blob-like structures for the density and temperature fields, while the vorticity displays a dipolar structure as expected from theory and experiment (cf. Ref. [8]). From such animations and radial correlations we find that the radial propagation velocity of the blob structures corresponds to around $0.05c_s$ consistent with Fig. 4, but with a large statistical variance in agreement with experimental measurements [2, 5, 6].

By combining the conditional evolution of n and v_x in Fig. 4 we deduce that the blobs are carrying a large particle flux. We have examined the PDF of the particle flux averaged over the periodic y -direction (the flux surface) at different radial positions. The PDF's are quite similar and strongly skewed with a flat exponential tail towards positive flux events, showing that the flux is dominated by strong bursts. The tail of the PDF was found to be well fitted by an extreme value distribution [13]. By coarse graining the PDF as described above we observe a similar behavior as for the local density fluctuations: the distribution approaches a Gaussian for large time scales.

We have demonstrated that a two-dimensional model for interchange turbulence provide results in good agreement with that reported from experimental investigations of SOL turbulence and transient transport events [2, 5, 6]. An important feature of the model is the spatial separation between forcing and damping regions. Our results are in quantitative agreement with experimental measurements of field-aligned blob-like structures propagating far into the scrape-off layer. The associated intermittent transport may have severe consequences for magnetic confinement experiments by producing large heat bursts on plasma facing components.

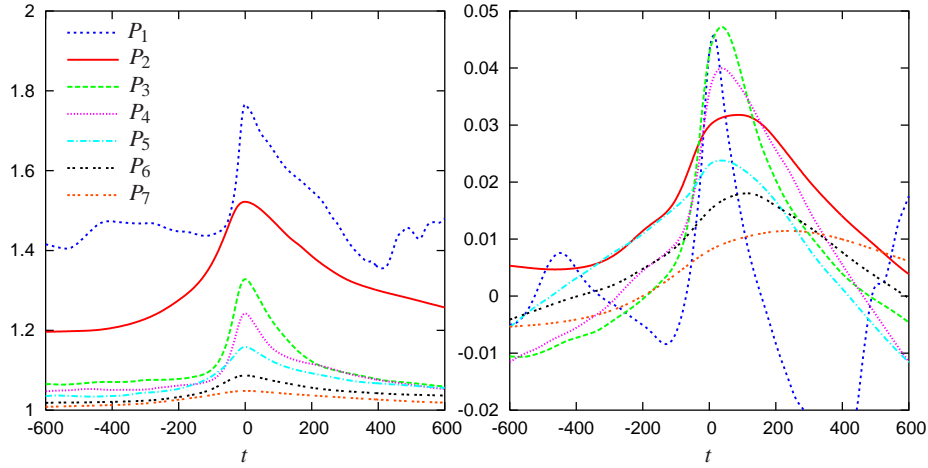


Figure 4: Conditionally averaged wave forms of the particle density (left panel) and the radial velocity v_x measured at seven different radial positions P_i as shown in Fig. 1, using the condition $n(x_{P_i}) - \bar{n}(x_{P_i}) > 4n_{\text{rms}}(x_{P_i})$.

This work was supported by the Danish Center for Scientific Computing through grants no. CPU-1101-08 and CPU-1002-17. O. E. Garcia has been supported by financial subvention from the Research Council of Norway.

References

- [1] T. Huld *et al.*, Phys. Fluids B **3**, 1609 (1991).
- [2] G. Y. Antar *et al.*, Phys. Plasmas **10**, 419 (2003); *ibid.* **8**, 1612 (2001); Phys. Rev. Lett. **87**, 065001 (2001).
- [3] M. Endler *et al.*, Nucl. Fusion **35**, 1307 (1995).
- [4] V. Antoni *et al.*, Phys. Rev. Lett. **87**, 045001 (2001).
- [5] J. A. Boedo *et al.*, J. Nucl. Mater. **313–316**, 813 (2003); Phys. Plasmas **10**, 1670 (2003); *ibid.* **8**, 4826 (2001) D. L. Rudakov *et al.*, Plasma Phys. Control. Fusion **44**, 717 (2002).
- [6] J. L. Terry *et al.*, Phys. Plasmas **10**, 1739 (2003); S. J. Zweben *et al.*, *ibid.* **9**, 1981 (2002); R. J. Maqueda *et al.*, *ibid.* **8**, 931 (2001).
- [7] S. I. Krasheninnikov, Phys. Lett. A **283**, 368 (2001); D. A. D’Ippolito *et al.*, Phys. Plasmas **9**, 222 (2002); N. Bian *et al.*, *ibid.* **10**, 671 (2003).
- [8] O. E. Garcia *et al.*, Phys. Rev. Lett. **92**, 165003 (2004).
- [9] O. E. Garcia *et al.*, Plasma Phys. Control. Fusion **45**, 919 (2003).
- [10] O. E. Garcia and N. H. Bian, Phys. Rev. E **68**, 047301 (2003).
- [11] V. Naulin *et al.*, Phys. Plasmas **10**, 1075 (2003).
- [12] V. Carbone *et al.*, Phys. Plasmas **7**, 445 (2000); R. Trasarti-Battistoni *et al.*, Phys. Plasmas **9**, 3369 (2002).
- [13] V. Naulin *et al.*, Phys. Lett. A **321**, 355 (2004).